SI Appendix 1

Partition Function and Free Energy Minimization

Here we provide more details of our statistical mechanical formulation.

Using Eq. **2** for the total partition function $Q_{\rm tot}$ and applying Stirling's approximation for the factorial (1),

$$\ln x! \approx x \ln x - x + \frac{1}{2}\ln(2\pi x) \ , \qquad [\mathbf{9}]$$

to the Helmholtz (canonical ensemble) free energy $A = -k_{\rm B}T \ln Q_{\rm tot}$, the per-ligand free energy in units of $k_{\rm B}T$ may be written as

$$\begin{aligned}
\frac{A}{N_l k_{\rm B}T} &= -\frac{1}{N_l}\ln Q_{\rm tot} \\
&= -\frac{N_c^{(b)}}{N_l}\ln\left(Q_c^{(b)}V\right) - \frac{N_r^{(f)}}{N_l}\ln\left(Q_r^{(f)}V\right) - \frac{N_l^{(f)}}{N_l}\ln\left(Q_l^{(f)}V\right) \\
&\quad + \frac{N_c^{(b)}}{N_l}\ln N_c^{(b)} - \frac{N_c^{(b)}}{N_l} + \frac{N_r^{(f)}}{N_l}\ln\left(N_r^{(f)}\right) \\
&\quad - \frac{N_r^{(f)}}{N_l} + \frac{N_l^{(f)}}{N_l}\ln N_l^{(f)} - \frac{N_l^{(f)}}{N_l} \ , \qquad [\mathbf{10}]
\end{aligned}$$

where we have omitted $[\ln(2\pi N_c^{(b)}) + \ln(2\pi N_r^{(f)}) + \ln(2\pi N_l^{(f)})]/(2N_l)$ because when $N_l \gg 1$, these contributions are negligible in comparison to the listed terms. The $N_l \gg 1$ condition is satisfied by the experimental system we aim to model. ($N_c^{(b)}$, $N_l^{(f)} \leq N_l$ by definition, and $N_r^{(f)} \leq N_l$ for $\gamma = 1$.)

Using the definitions in the main text for θ and γ and noting that $N_r^{(f)}/N_l = \gamma - \theta$, we cast the above equation in the form of

$$\begin{aligned}
\frac{A}{N_l k_{\rm B}T} &= \theta \ln \frac{\theta}{Q_c^{(b)}} + (\gamma - \theta)\ln\frac{(\gamma-\theta)}{Q_r^{(f)}} \\
&\quad + (1-\theta)\ln\frac{1-\theta}{Q_l^{(f)}} + (1+\gamma-\theta)\left(\ln\rho_l - 1\right) \ . \qquad [\mathbf{11}]
\end{aligned}$$

This free energy takes into account all possible configurations and dictates their relative statistical weights. In general, the properties of a system are determined by Boltzmann averaging over all possible configurations. However, if the configuration distribution over a certain variable is sharply peaked, the behavior of the system is well approximated by that of the most probable configuration for that variable. We are primarily interested in the fraction of ligands bound, θ. The most probable θ is determined by minimizing A, i.e., requiring

$$\frac{\partial}{\partial\theta}\frac{A}{N_l k_{\mathrm{B}} T} = 0 \; . \qquad [\mathbf{12}]$$

Applying this condition to Eq. **11** leads to

$$0 = -\ln Q_c^{(b)} + \ln Q_r^{(f)} Q_l^{(f)} + \ln \frac{\theta}{(1-\theta)\,(\gamma-\theta)} - \ln \rho_l \; . \qquad [\mathbf{13}]$$

This is a quadratic equation in θ,

$$\frac{(1-\theta)\,(\gamma-\theta)}{\theta} = \frac{Q_r^{(f)} Q_l^{(f)}}{Q_c^{(b)} \rho_l} \; , \qquad [\mathbf{14}]$$

that can be readily solved to yield Eq. **3**. The other solution for θ is discarded because for $Q_r^{(f)} Q_l^{(f)} / Q_c^{(b)} \rho_l > 0$ (which always holds) and irrespective of γ, it always gives $\theta > 1$ which contradicts the definition of θ requiring it to be ≤ 1.

How representative is the most probable θ for the behavior deriving from the ensemble encompassing all possible configurations? We have tested the accuracy of the $\partial A/(N_l k_{\mathrm{B}} T)/\partial\theta = 0$ approximation for the $\gamma = 1$ case. When $\gamma = 1$, Eq. **11** may be rewritten as

$$\frac{A(\theta)}{N_l k_{\mathrm{B}} T} = \ln \left[\left(\frac{Q_r^{(f)} Q_l^{(f)}}{Q_c^{(b)}} \right)^{\theta} \theta^{\theta} \, (1-\theta)^{2(1-\theta)} \right] + (2-\theta)\,(\ln \rho_l - 1) - \ln Q_r^{(f)} Q_l^{(f)} \; , \qquad [\mathbf{15}]$$

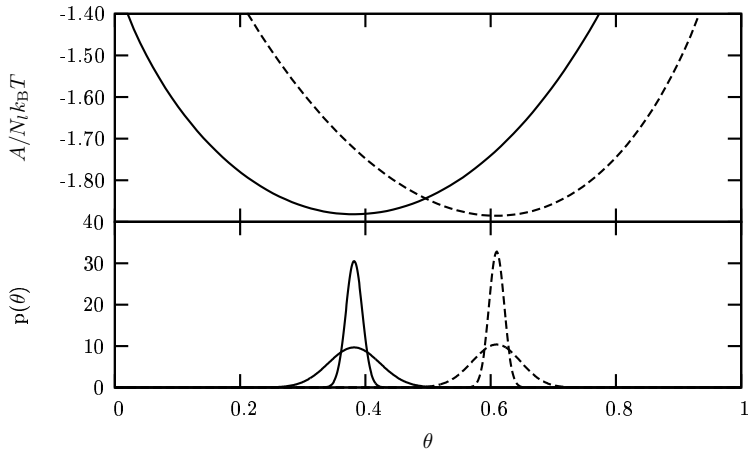

Fig. 5. An example calculation illustrating the accuracy of the $\partial A/(N_l k_B T)/\partial\theta = 0$ free energy minimization approximation. The upper and lower panels show, respectively, $A(\theta)/(N_l k_B T)$ and probability density $p(\theta)$ as a function of θ for $\rho_l = 0.5K_d$ (solid curves) and $\rho_l = 2.0K_d$ (dotted curves). $p(\theta)$ is shown for $N_l = 10^2$ (broad peaks) and $N_l = 10^3$ (sharp peaks).

where the last term $Q_r^{(f)}Q_l^{(f)}$ is independent of θ. Using this relation, we have verified that for sufficiently large N_l, the configurational population distribution over θ is sharply peaked, and therefore the most-probable-θ approximation is reasonably accurate (SI Fig. 5). In a more extensive analysis (data not shown), we have also verified numerically that $\Delta\theta$, the full width at half maximum of the $p(\theta) = \exp[-A(\theta)/k_B T]$ distribution, decreases with increasing N_l and scales in accordance with $\Delta\theta \sim 1/\sqrt{N_l}$ as expected.

Polyampholytic Effects: Polarizable Charge Distribution of a Disordered Ligand Can Enhance Binding Affinity

Our analysis in the main text has been based on the simplifying assumption that the charge distribution of the disordered ligand remains unchanged upon binding. This assumption is useful as a first approximation, but is limiting. While we will leave in-depth analyses using higher-resolution chain modeling to future work, it is instructive to explore here how possible adjustments of charge distribution might impact binding affinity. A defining characteristic of the disordered ligands of interest here is that they are polyampholytes — polymer molecules with both positive and negative charges (2, 3). In general, because of an induced dipole effect, the polarizable charge distribution of a disordered polyampholyte can lead to stronger attractive electrostatic interactions with charged objects. For instance, a semi-quantitative scaling argument stipulates that an overall neutral polyampholytic chain is attracted to a charged sphere by an interaction energy $\sim -(r_c/\langle r\rangle)^4$, where $\langle r\rangle$ is the separation between the charged sphere and the center of mass of the polyampholyte and r_c is a cross-over separation at which the polyampholyte deviates from an overall Gaussian shape (4).

As an illustration of such an effect, we consider here a toy model describing the interaction between a sphere of charge q_r (> 0) and a Gaussian chain containing two effective charges, $+q$ and $-q$ ($q \geq 0$) separated by a distance l, the average value of which is l_0 when $q = 0$ and $q_r = 0$ (Fig. 6*A*). Thus, $l_0 \sim \sqrt{N}$, where N is the (contour) length of the polymer chain (5) connecting the $\pm q$ effective charges. Deviation of l from l_0 entails deformation of the Gaussian chain distribution and thus an unfavorable decrease in chain conformational entropy. Theory for rubber elasticity (6) suggests that this effect may be captured approximately by a free energy term $\sim [(l - l_0)/l_0]^2$. We include this contribution as part of an effective interaction energy of the

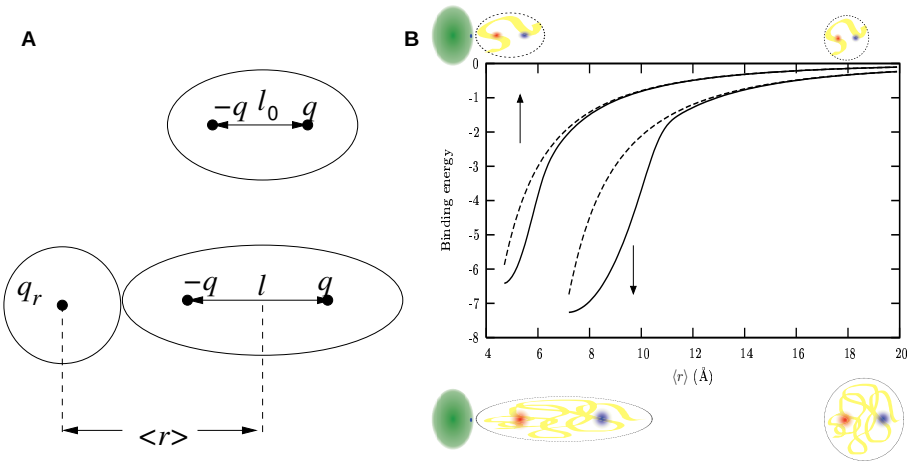

Fig. 6. A toy model for polyampholytic effects in the binding of a disordered protein. (A) Schematics of a flexible Gaussian chain in the free state (upper drawing) and when it is bound to a charged sphere at a distance $\langle r\rangle$ from the center of the chain (lower drawing). Note that the average distance in the free state between the $\pm q$ effective charges, for $q \neq 0$, will be $< l_0$ because of electrostatic attraction between them. (B) Binding energy (see text) as a function of $\langle r\rangle$ for Gaussian chains with an average spatial separation between the two charges equals to $l_0 = 5$ Å (upper two curves) and $l_0 = 10$ Å (lower two curves) when each of the chains is far away from other charges. For each l_0, the binding energy is shown for both a stiff chain (dashed curves – weaker bound, higher binding energy) and a flexible chain (solid curves – tighter bound, lower binding energy). The following numerical parameters are used in this example: $q = 0.1$, $q_r = 3$, $\alpha = 0.1$, $\sigma = 10$, $e_{\rm rep} = 0.1$, and $r_{\rm rep} = 1$. Distance and energy are in Å and kcal/mol, respectively.

model system:

$$
\begin{aligned}
E_{\rm eff}(q_r;\langle r\rangle, l \;\; = \;\; & \frac{-qq_r}{\epsilon_d(\langle r\rangle - l/2)} e^{-\alpha(\langle r\rangle - l/2)} + \frac{qq_r}{\epsilon_d(\langle r\rangle + l/2)} e^{-\alpha(\langle r\rangle + l/2)} \\
& - \frac{q^2}{\epsilon_d l} e^{-\alpha l} + \sigma \left(\frac{l - l_0}{l_0}\right)^2 \\
& + e_{\rm rep}\left[(l - r_{\rm rep})^{-12} + (\langle r\rangle - l/2 - r_{\rm rep})^{-12}\right] \;, \qquad \textbf{[16]}
\end{aligned}
$$

where $\sigma \sim T$ may be treated as a constant because the present analysis

does not consider temperature dependence, and an excluded-volume radius r_{rep} as well as a repulsive energy parameter e_{rep} are introduced to provide a crude account of chain excluded volume effects. For simplicity, a single dielectric constant $\epsilon_d = 5.0$ is used for all three electrostatic terms. We determine the average effective interaction energy $\langle E_{\mathrm{eff}}(q_r; \langle r \rangle) \rangle$ between the charge sphere and the Gaussian chain at a given center-of-mass separation $\langle r \rangle$ by performing a Boltzmann average of $E_{\mathrm{eff}}(q_r; \langle r \rangle, l)$ over l at $T = 298$ K. The binding energy as a function of center-of-mass separation between the charged sphere and the Gaussian chain is then given by $\langle E_{\mathrm{eff}}(q_r; \langle r \rangle) \rangle - \langle E_{\mathrm{eff}}(q_r = 0; \langle r \rangle) \rangle$. Fig. 6*B* compares the results from this toy model for a flexible chain with polarizable charge distribution (l allowed to vary) and a stiff chain with a fixed charge distribution (l fixed at l_0, corresponding to $\sigma \to \infty$), and how this difference in behavior is affected by the chain length between the $+q$ and $-q$ effective charges.

Fig. 6*B* shows that, at small $\langle r \rangle$, flexible polymers can adjust l so that the binding energy becomes more favorable than if the polymers are stiff. Owing to their higher degrees of conformational freedom, the longer polymer can gain more energetic favorability (more negative binding energy) through conformational deformation than the shorter polymer. The binding energy of the longer polymer is also consistently more favorable both for the stiff and for the flexible cases, because of the larger separations $\langle r \rangle + l$ between q_r and $+q$, and hence less Coulombic repulsion between this pair of positive charges.

These results are broadly consistent with a K_d for 7-fold phosphorylated Sic1 (1-90) of ~ 1 μM (T.M., W.-Y. Choy, S. Orlicky, F. Sicheri, L. Kay, M.T., and J.D.F.-K., unpublished data). Using the same model parameters as for those of the short peptides underestimates the affinity. Thus, it is expected that polarization effects within the full-length Sic1 will be important for tight binding.

1. Arfken G (1970) *Mathematical Methods For Physicists* (Academic, London), 2nd Ed.

2. Doty P, Imahori K, Klemperer E (1958) *Proc Natl Acad Sci USA* 44:424–431.

3. Higgs PG, Joanny JF (1991) *J Chem Phys* 94:1543–1554.

4. Dobrynin AV (2001) *Phys Rev E* 63:051802.

5. Cantor CR, Schimmel PR (1980) *Biophysical Chemistry* (Freeman, New York).

6. Flory PJ (1953) *Principles of Polymer Chemistry* (Cornell Univ Press, Ithaca, NY).